Effect of Particle Size Segregation in Debris Flow Deposition: A Preliminary Study

Lu Jing[1,2], Fiona C. Y. Kwok[1,2*], Tao Zhao[2], and Jiawen Zhou[2]

[1] Department of Civil Engineering, The University of Hong Kong, Pokfulam Road, Hong Kong
[2] State Key Laboratory of Hydraulics and Mountain River Engineering, College of Water Resource and Hydropower, Sichuan University, Sichuan, 610065, China
*fiona.kwok@hku.hk

Abstract. To understand the effect of size segregation in the depositional process of debris flows, both flume experiments at the laboratory scale and numerical simulations using the discrete element method (DEM) are performed. A variety of particle size distributions with coarse and fine particles are adopted. It is found that larger particles tend to reach the front of the final deposits, while small particles are accumulated at the tail of the flows. Quantitative agreement is achieved in the DEM simulations, where rolling resistance and geometric roughness at boundaries are adopted to account for the effect of particle shape. With the DEM results, the effect of segregation on the runout distance is studied from the perspective of energy dissipation. The progress of segregation is analyzed in detail, which revealed that segregation occur slowly while the flow is propagating rapidly over the slopes; it becomes significant during the deposition stage, where more large particles are found near the surface. The effect of segregation in debris flow deposition can help better predict the runout distance and impact pressure, which is crucial in the assessment and mitigation of debris flow-related natural hazards.

Keywords: Segregation, Debris flow, Flume experiment, DEM.

1 Introduction

Particle size segregation can be found in debris flows where coarse and fine grains tend to separate themselves according to their different sizes [1]. In general, small particles settle towards the bottom while large particles drift towards the surface [2–4]. The occurrence of such segregation may enhance the runout distance and modify the deposit morphology, which are crucial in the assessment and mitigation of debris flow-related natural hazards [5–8].

To understand the effect of size segregation in the depositional process of debris flows, both flume experiments at the laboratory scale and numerical simulations using the discrete element method (DEM) are performed. Our focus is the effect of flow composition (i.e., particles size distributions) on flow dynamics, thus runout distance and deposit morphology. In the current preliminary work, we report a set of experi-

ments with different concentrations of large and small particles, and propose a DEM model which captures the main flow behaviors by using spherical particles, rolling friction, and a dissipative base with geometric roughness. By calibrating input parameters independently for each species (i.e., large and small grains), the segregating behavior of the mixture of large and small grains can be reproduced without further calibration. The effects of segregation on the flow dynamics and deposit morphology are discussed.

2 Experiments and Simulations

2.1 Experimental Setup

The experimental flume consists of a channel with two inclined segments and a horizontal part, as shown in Fig. 1. The upper and lower slopes have the length of 2 m and 1.5 m, and the angles of inclination of 38.3° and 17.5°, respectively. A tank (0.5 m long) is located at the top of the flume. The width of the whole channel is consistently 0.35 m. In this paper, we define the start of the horizontal channel as $x = 0$, x-axis points along the runout direction, and the z-axis points upward.

The materials we use are rock fragments taken from a site of natural debris avalanche in the Bayi Gully, Southwest China [9]. The size of "large" gains varies between 40 mm and 60 mm, while "small" grains are 10–20 mm in diameter. In this paper we report the results of four experiments, each has a different mass concentration of large grains, i.e., $\Phi_L = 0$, 33.3%, 66.7% and 100%. In each experiment, dry rock fragments with a total mass of 60 kg is well mixed and poured into the tank. The gate of the tank is removed quickly to initiate the flow, which accelerates on the upper slope and deposit on the lower regions. After the cease of each flow, we measure the weight of large and small grains every 0.2 m along the channel, producing accumulative percentage of mass for large, small, and all grains.

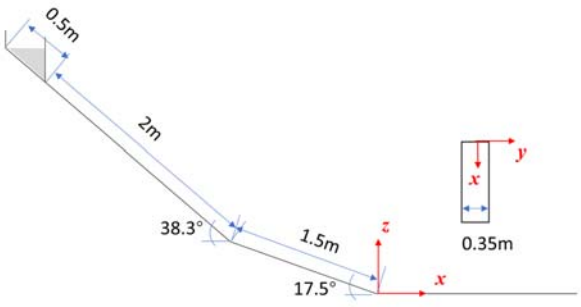

Fig. 1. Flume and coordinate system.

2.2 Numerical Model

Discrete element modeling of the experimental debris flows is performed using an opensource program, LIGGGHTS, which implements the Hertz model for the calculation of contact forces [10]. In this model, four material properties are used, namely, Young's modulus E, Poisson's ratio ν, the coefficient of friction μ, and the coefficient of restitution e.

We use spherical particles with uniform size distribution to model the large (40–60 mm) and small (10–20 mm) grains. The initial mass of each test is reproduced, as shown in Fig. 2. Note that due to the effect of gravity, a slight initial separation of the two species can be observed for the 33.3% and 66.7% cases. However, such an initial segregation is negligible compared to the major segregation stages, as we shall see in the later analysis.

A layer of spherical beads is fixed as a rough bed on the surface of the entire channel [11]. Although in the experiments the bottom is made of flat plane, the roughened base is necessary in the DEM simulations due to the use of spherical particles. This treatment introduces several parameters, such as the size/distribution of base particles, and the contact parameters between the fixed and flowing particles. In this work, we arrange the base particles with a triangular close packing, and the particles size is set as 10 mm (see Fig. 2(e)). The choice makes sure that large grains can slide over the base layer, while small grains can accumulate at a lower slope, consistent with the experimental observations. The contact parameters between the flow and the boundary particles will be adjusted to match the experimental results, as presented later.

Another necessary treatment resulting from the use of spherical particles is to employ a rolling friction model in the flowing particles. A rolling friction parameter, μ_r, is used to account for the shape effect, which will be calibrated in the next section.

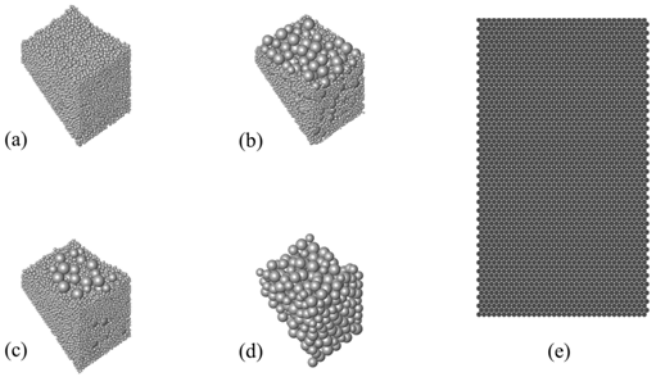

Fig. 2. Numerical models. (a–d) The initial mass of 60 kg with an overall mass concentration of large particles 0, 33.3%, 66.7% and 100%, respectively. (e) The triangular arrangement of base particles with a size of 0.01m over the whole channel bottom.

2.3 Calibration and Validation

Our uniaxial compression tests on single grains suggest a stiffness of 50 kN/mm. In the DEM model we use $E = 10^9$ Pa and $\nu = 0.25$ for all particles, and we have verified that the results are not sensitive to these parameters. The tested angles of repose for large and small grains vary in a range of 31–36°, based on which we choose μ =0.5 and μ_r = 0.2, which produce reasonable results in terms of the overall kinetics gained during each test. Since the collective behavior of a dense granular flow is not significantly affected by the coefficient of restitution, we choose a low value of e = 0.2 to avoid unphysical collisions for the highly-energetic frontal grains.

As the major parameters are chosen, we fine-tune the coefficient of friction between flowing particles and base particles, μ_b, to match the final deposit in the two cases with only small and large grains, respectively. Good agreement is achieved for both species with μ_b = 0.18. The experimental and numerical deposits of the Φ_L = 0 case (i.e., only small grains) are presented in Fig. 3, which show a similar depositional behavior at the toe of the lower slope. In Fig. 4(a) we plot the comparison of cumulative percentage of each species (i.e., large and small grains) when μ_b = 0.18 is used. In general, the deposit morphology is captured. However, note that a large discrepancy appears at the front of the coarse-grain case. This is attributed to the fact that when large grains at the front leave the bulk, they can continue running for a longer distance than that in the experiment (where grains come to a halt easily due to shape effect). We mark these regimes of runny grains with the dashed lines in Fig. 4, which represent where only isolated grains present. The dash lines show that the discrepancy between numerical and experimental results mainly occur at these regimes.

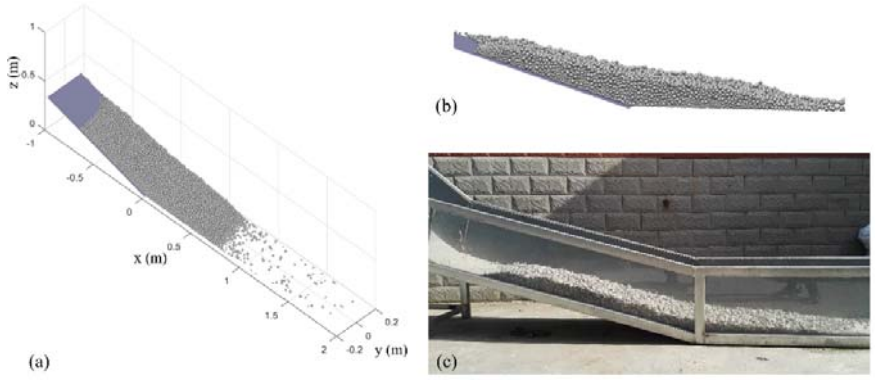

Fig. 3. Calibration of the Φ_L = 0 case (purely small grains). (a) The final deposit in numerical simulation. (b) Side-view numerical deposit. (c) Side-view experiment deposit.

The value (i.e., μ_b = 0.18) obtained through independent calibrations of the two species is then applied in the mixture cases where both large and small grains exist (i.e., Φ_L = 33.3% and 66.7%). As expected, the overall depositional behaviors can be cap-

tured without further adjustment of parameters (Fig. 4(a)), and more importantly, the segregation behaviors are also well reproduced (Fig. 4(b)). By comparing the two panels in Fig. 4, it is clear that larger particles tend to reach the front of the final deposits, while small particles are accumulated at the tail of the flows.

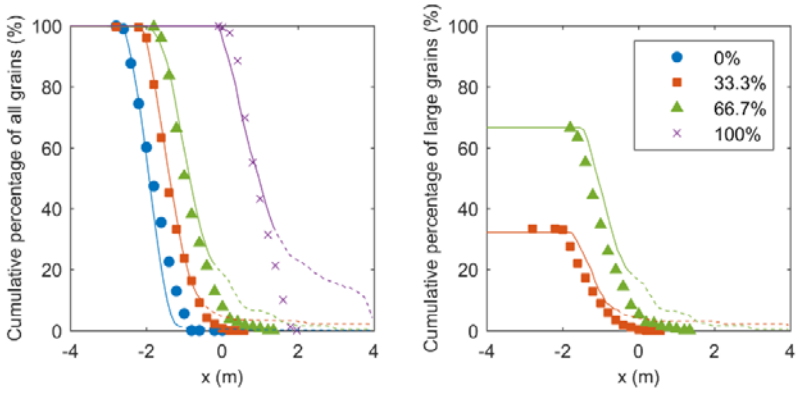

Fig. 4. Validation of numerical simulations by comparing the cumulative mass percentage of all (left panel) and large (right panel) grains along the channel. Symbols and lines are experimental and numerical results, respectively; colors and symbol types are explained in the legend. The dash lines represent frontal regions where grains remain loosely contacted (see text).

3 Results

3.1 Flow Dynamics

As seen in Fig.4, despite the same initial mass (60 kg), thus the same potential energy, the runout distance is largely affected by the composition of debris flows. The case with purely large grains reaches a much longer distance after running out of the inclined channel. As the mass of small particles increases, the runout decreases.

Figure 5 shows the temporal evolution of the average kinetic energy, $\langle E_k \rangle$, for each case. Note that the vertical axis is in log scale. In the early stage (t < 2 s), the grains in the Φ_L = 100% case gain an average kinetic energy which is greater than the other cases by a factor of 50–100. In other words, the energy dissipation increases significantly with the increasing number of small particles. We attribute this particle size dependency of energy dissipation to the number of particle–particle contacts [12]. Indeed, more contacts occur in a flow of more small particles, given the same total mass, thus a higher dissipation of energy through sliding and collisions. As we can observe from both the experiments and simulations, the Φ_L = 100% case presents a loose state where grains remain poorly connected until they start to deposit, while the flow in other cases is generally dense due to the presence of a large number of small grains. To demonstrate this, in Fig. 6 we plot the coordination number, Z, for each flow, which measures the average number of contacts. In the initial state, all cases

have $Z > 4$. It drops dramatically towards zero since the materials start to flow. When the flow reaches a slower slope or the horizontal region, deposition occurs and the number of contacts start to increase. However, Z only increases to a value below 2 in the $\Phi_L = 100\%$, showing that the large grains therein are not flowing in a dense state.

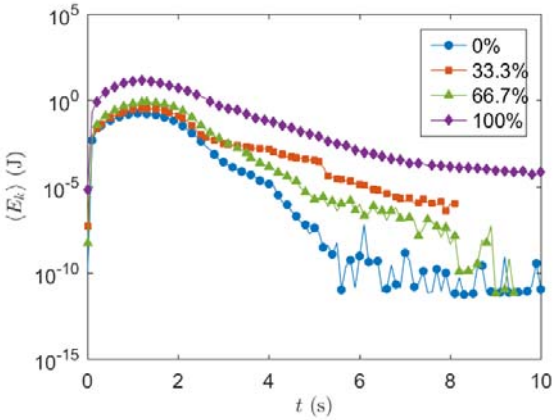

Fig. 5. Evolution of the average kinetic energy ($\langle E_k \rangle$) with time (t).

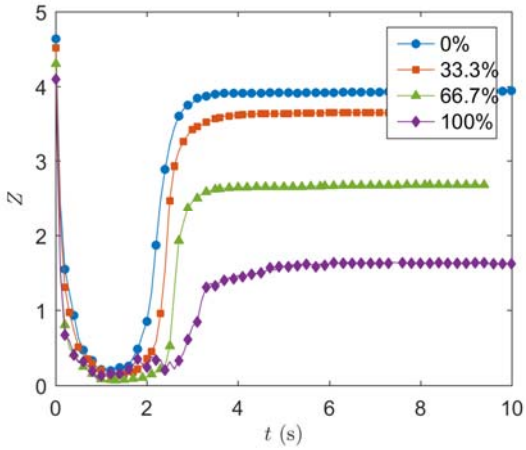

Fig. 6. Evolution of the average number of contacts (Z) with time (t).

3.2 Process of Segregation

Next, we analyze the process of segregation in the two mixture cases, i.e., Φ_L = 33.3% and 66.7%. To monitor the occurrence of segregation, we divide the flow at

any moment as vertical bins with a width of 0.5 m. In each bin (No. i), we calculate the normalized (by local flow thickness) centers of mass for large and small particles, which are denoted as C_L^i and C_s^i, respectively. The local degree of segregation is then defined as $\alpha^i = (C_L^i - C_s^i) + 0.5$. The addition of 0.5 is to define $\alpha_i = 0.5$ as the initial state when $C_L^i = C_s^i$. The overall degree of segregation, α, is calculated by averaging over all bins where both large and small particles exist. Standard deviation is also recorded as the averaging step is performed, which represents the deviation of the state of segregation at different locations.

Figure 8 shows the progress of segregation in the two mixture cases. As we noted in Fig. 2, a small amount of segregation already occurs in the initial state during the sample generation, which is however negligible compared to the later stage where α is close to 1. The standard deviation indicated by the length of error bars is the greatest before deposition occurs (around 2 s). When most of the flow is on the slopes, segregation takes place slowly. Segregation becomes more significant in the deposition stage, where nearly all large particles emerge on the surface.

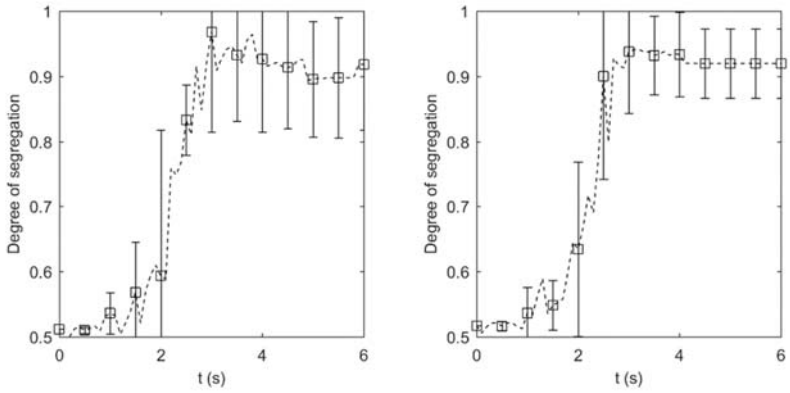

Fig. 7. Progress of segregation. Left: Φ_L=33.3%. Right: Φ_L=66.7%.

4 Concluding Remarks

In this paper, flume experiments and DEM simulations are performed to understand the effect of segregation in the deposition process of debris flow. The flow dynamics and the progress of segregation are analyzed. The work is a preliminary study towards a better understanding of segregation in debris flow-like natural hazards. Future work will focus on creating experimental debris flows that are more relevant to natural debris flows, and exploring the energy dissipations in relation to particle size distribution and the mechanical aspects of segregation with the aid of DEM modeling.

References

1. C. G. Johnson, B. P. Kokelaar, R. M. Iverson, M. Logan, R. G. LaHusen, and J. M. N. T. Gray. Grain-size segregation and levee formation in geophysical mass flows. Journal of Geophysical Research, 117, F1 (2012).
2. S. B. Savage and C. K. K. Lun. Particle size segregation in inclined chute flow of dry cohesionless granular solids. Journal of Fluid Mechanics, 189, 311–335 (1988).
3. J. M. N. T. Gray and A. R. Thornton. A theory for particle size segregation in shallow granular free-surface flows. Proc. R. Soc. A, 461(2057), 1447–1473 (2005).
4. L. Jing, C. Y. Kwok, and Y. F. Leung. Micromechanical Origin of Particle Size Segregation. Phys. Rev. Lett., 118 (11), 118001 (2017).
5. B. P. Kokelaar, R. L. Graham, J. M. N. T. Gray, and J. W. Vallance. Fine-grained linings of leveed channels facilitate runout of granular flows. Earth and Planetary Science Letters, 385, 172–180 (2014).
6. Zanuttigh, B., Lamberti, A. Instability and surge development in debris flows. Review of Geophysics. 45(3), 2005RG000175 (2007).
7. G. G. D. Zhou and C. W. W. Ng. Numerical investigation of reverse segregation in debris flows by DEM. Granular Matter, 12(5): 507-516 (2010).
8. G. G. D. Zhou, N. G. Wright, Q. C. Sun, and Q. P. Cai. Experimental Study on the Mobility of Channelized Granular Mass Flow. Acta Geologica Sinica. 90(3):988-998 (2016).
9. J. Zhou, K. Huang, C. Shi, M. Hao, and C. Guo. Discrete element modeling of the mass movement and loose material supplying the gully process of a debris avalanche in the Bayi Gully, Southwest China. Journal of Asian Earth Sciences, 99, 95–111 (2015).
10. C. Goniva, C. Kloss, N. G. Deen, J. A. M. Kuipers, and S. Pirker. Influence of rolling friction on single spout fluidized bed simulation. Particuology, 10(5), 582–591 (2012).
11. L. Jing, C. Y. Kwok, Y. F. Leung, and Y. D. Sobral. Characterization of base roughness for granular chute flows. Physical Review E, 94(5), 052901 (2016).
12. S. Utili, T. Zhao, and G. T. Houlsby. 3D DEM investigation of granular column collapse: Evaluation of debris motion and its destructive power. Engineering Geology, 186, 3–16, (2015).